Published in "Journal of Physics B: Atomic, Molecular And Optical Physics
36(12): 2489-2500, 2003"
which should be cited to refer to this work.

Threshold peaks and structures in elastic and vibrationally inelastic electron impact cross sections for CS_2

Michael Allan

Department of Chemistry, University of Fribourg, Pérolles, CH-1700 Fribourg, Switzerland

Abstract

Elastic, vibrationally inelastic and superelastic cross sections were measured for electron impact on CS_2 at 135°, with emphasis on the threshold region. The elastic cross section rises dramatically at low energies. The cross sections for the excitation of all three fundamental vibrations (010), (100) and (001) have very strong threshold peaks, more than ten times higher than those observed for CO_2. The elastic and the (010) and (100) inelastic cross sections have deep narrow structures at energies up to about 0.3 eV. The structures are weak for the (001) vibration. Substantial excitation of overtone vibrations is observed even near threshold. The threshold structures appear to be caused primarily by the $^2\Pi_u$ valence state of CS_2^-. Various broad resonant peaks are observed in the cross sections in the 1–12 eV range.

(Some figures in this article are in colour only in the electronic version)

1. Introduction

The present study is concerned with threshold peaks and structures in CS_2, in particular in comparison with those observed in CO_2. Threshold peaks in vibrational excitation of molecules by electron impact, discovered more than 25 years ago by Rohr and Linder (1976) in hydrogen halides, are large enhancements of cross sections in a narrow region above the threshold. Threshold peaks and near-threshold structures in hydrogen halides have recently been studied in greater depth, taking advantage of improved experimental techniques and advances in theory, describing scattering in terms of a nonlocal complex potential (Allan *et al* 2000, Čížek *et al* 2001, 2003, Hotop *et al* 2003).

The threshold peaks were originally found in polar molecules, where the dipole moment plays a decisive role by binding an electron at intermediate internuclear distances, larger than the equilibrium internuclear distance of the neutral molecule. They have subsequently also

been found in nonpolar molecules, in particular in the excitation of the symmetrical stretch vibration in CO_2, where they have been ascribed to a virtual state of the anion (Morgan 1998, Estrada and Domcke 1985, Kochem *et al* 1985, Field *et al* 1991). In CO_2 the threshold peak is found for the upper member of the Fermi dyad containing the symmetrical stretch (Allan 2001a). Related to the threshold peaks are narrow dips or peaks in the cross sections found at or slightly below the vibrational thresholds, for example in HF, and ascribed to vibrational Feshbach resonances (Knoth *et al* 1989, Čížek *et al* 2003). At higher energies the Feshbach resonances become broader and gradually turn into wavy oscillations; the boomerang structure. Narrow structures were recently, somewhat unexpectedly, also observed in CO_2 (Allan 2002). They were ascribed to the fact that the virtual state calculated in linear geometry becomes an electronically bound state (for fixed nuclei) when CO_2 is bent and stretched, as predicted theoretically by Tennysson and Morgan (1999). This electronically bound portion of the CO_2^- potential surface supports vibrational Feshbach resonances. The interpretation is supported by the high-level calculations of the bound part of the CO_2^- potential surface by Sommerfeld (2003).

CS_2 is isovalent with CO_2. Like CO_2 it does not have a permanent dipole moment, but is much more polarizable (59.4 a_0^3 compared with 19.4 a_0^3 for CO_2, Lide (1995)). Its study could thus shed some light on the role of polarizability on threshold peaks and structures. Absolute cross sections for electron scattering on CS_2 are, furthermore, relevant for discharge physics. Absolute differential cross sections in CS_2 have been measured by Sohn *et al* (1987) for a number of discrete energies between 0.3 and 5 eV. A preliminary account of the present study reported deep narrow structures in the elastic and vibrationally inelastic cross sections (Allan 2001b, 2001c). Deep structures were also found by Jones *et al* (2002) in their very low energy and very high resolution measurements of the total integral and backward cross sections. They were interpreted in terms of giant resonances and symmetry selection rules. This paper presents a more detailed account of the measurements of the elastic and vibrationally inelastic differential cross sections at 135° with emphasis to the threshold region. A brief overview of the cross sections up to 12 eV is also given.

2. Experimental details

The measurements were performed using a spectrometer with hemispherical analysers which has already been described (Allan 1992, 1995). The response function of the spectrometer at very low energies has recently been improved by adding more degrees of freedom in compensating residual electric fields in the collision region. The resolution of the instrument has been improved using rectangular apertures defining the pupil, providing a ribbon-shaped beam in the analysers (Allan 2001a). The energy of the incident beam was calibrated on the 19.365 eV (Gopalan *et al* 2003) ^{2}S resonance in helium and is accurate to within ±20 meV. The elastic peaks in the energy loss spectra of figure 1 are 10.2 meV (bottom) and 11.1 meV (top) wide, indicating a resolution of 10–11 meV in energy loss, and 7–8 meV in the incident beam. The analyser response function was determined on the elastic scattering in helium. The sample inlet nozzle had a diameter of 0.25 mm and was kept at ∼30 °C during the measurements. Absolute values of the cross sections were determined by comparison with the elastic cross section of helium of Nesbet (1979) using the relative flow method.

The error limit is ±20% for the elastic cross section. The error limit of the cross sections for the excitation of the fundamental vibrations is larger, taken as ±40% at energies higher than about 70 meV above the threshold, and around ±50% within the first 70 meV above the threshold. The larger error of inelastic cross sections is caused by the additional assumption that the response function derived by measuring the elastic helium signal can also be applied

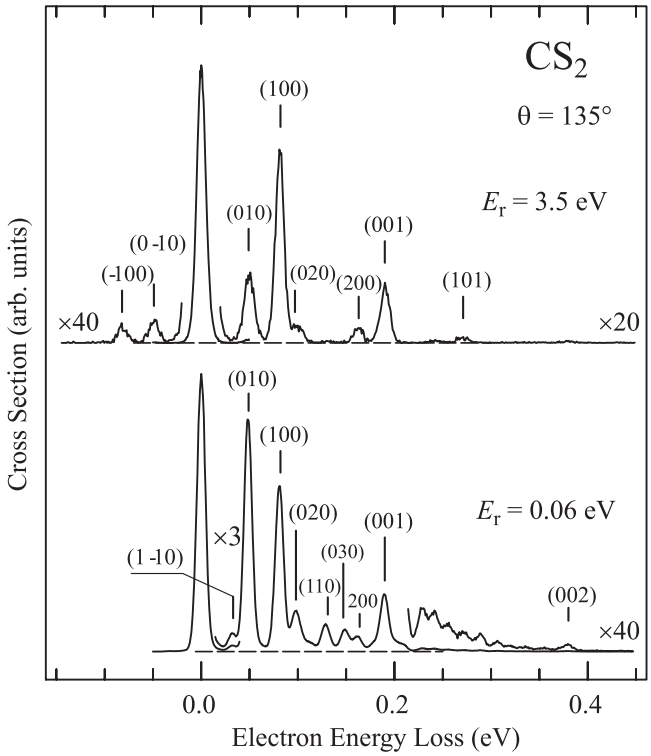

Figure 1. Electron energy-loss spectra recorded at the constant residual energies indicated. Negative numbers in the assignment indicate superelastic scattering from thermally vibrationally excited molecules where the corresponding vibrational quantum decreases in the transition. The elastic cross sections at 0.06 and 3.5 eV are 9.1 and 1.3 Å^2 sr^{-1}, respectively, indicating the relative intensities of the spectra in the lower and upper panels.

to inelastic excitation functions. This assumption is justified by the fact that the energy losses encountered in this work are quite small. The assumption is not quite correct, however, particularly at very low energies (<0.3 eV) because the incident beam becomes diffuse and the response function depends on both incident and residual energies. A better approximation would be the 'product rule' applied previously for the deeply inelastic cross sections in helium (Allan 1992), but not used here because of the difficulty of deriving separate monochromator and analyser response functions for vibrational excitation at very low energies. In addition, the thermal population of excited vibrational levels has been neglected in the interpretation of the present data, which consequently contains a contribution of 'hot' transitions. (That is, the (000) → (000) elastic cross section contains a contribution from (010) → (010), the (000) → (010) cross section a contribution from (010) → (020) transition, etc.) Future measurements of the temperature dependence of the spectra will be required to disentangle these contributions, in a way which has been demonstrated for CO_2 in the pioneering work of Johnstone *et al* (1993, 1999). The error of the cross sections for the excitation of the overtone and combination vibrations is even larger, because they are affected by band overlap. The error of the superelastic cross sections is estimated as ±40% at incident energies above about 140 meV, but increases dramatically at lower energies because of the rapidly deteriorating quality of the incident electron beam. It is around a factor of 2 in the 70–140 meV range, and the signal becomes only qualitative at incident energies below 70 meV.

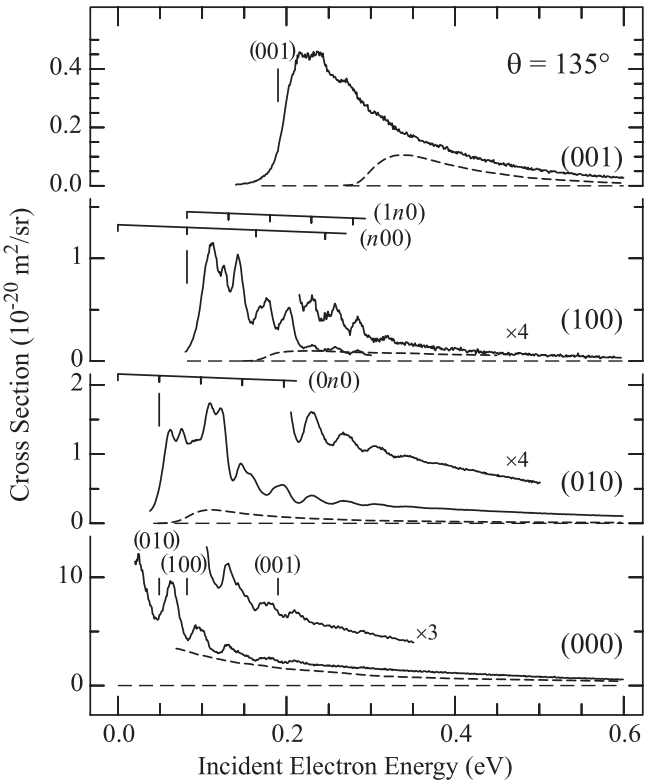

Figure 2. Differential cross sections for the final states indicated. The CO_2 cross sections (Allan 2001a, 2002) are shown for comparison as dashed curves. Selected vibrational thresholds are indicated by vertical bars and grids above the spectra.

3. Results at low energy

3.1. Energy-loss spectra

The energy-loss spectra shown in figure 1 were recorded by collecting scattered electrons with the fixed residual energies of $E_r = 0.05$ and 3.5 eV and varying the incident electron energy E_i. The abscissa shows the energy loss $\Delta E = E_i - E_r$, that is, the spectra scan through the various excitation energies of the target. All the bands in the lower spectrum were recorded very close to their respective excitation thresholds. The upper spectrum is characteristic of excitation at higher energies. All three vibrations are seen to be excited under both conditions. Comparison with spectra recorded under similar conditions in CO_2 (Allan 2001a) reveal a certain reversal of trends in terms of overtone excitation. Overtones are excited substantially at the threshold in CS_2 while they are very weak in CO_2. On the other hand, strong excitation of the (010) and (100) vibrations, including overtones, was observed with $E_r = 3.8$ eV in CO_2, while overtone excitation is weak with $E_r = 3.5$ eV in CS_2.

3.2. Elastic scattering and excitation of fundamental vibrations

Figure 2 shows the elastic and various inelastic cross sections for the incident electron energy E_i. Both E_i and E_r were scanned in this experiment, so as to keep the energy loss

ΔE fixed and equal to zero for the elastic scattering and equal to the appropriate excitation energy of the target for inelastic scattering. Near the threshold the elastic, and to an even more dramatic degree the inelastic cross sections are found to be larger in CS_2 than in CO_2. In addition, the elastic as well as the (010) and (100) inelastic cross sections have deep narrow structures. (The structure in the (001) cross section is much less pronounced.) This is in contrast to CO_2, where oscillatory structures were found in the near-threshold region in the excitation of certain overtone vibrations but not in the elastic cross section and the excitation of the fundamental vibrations (Allan 2002).

The present elastic cross section closely resembles the total cross section of Jones *et al* (2002) in terms of overall shape and the details of the structure. Hotop *et al* (2003) presented a comparison of the two data sets, under the assumption of an isotropic angular distribution. The present data yields an absolute magnitude that is about 30% smaller than that of Jones *et al* (2002); a reasonable agreement in view of the different natures of the two experiments and of the possibility of some anisotropy in the angular distribution.

The structures in CO_2 were found to lie at or (at higher electron energies) slightly below the thresholds for the excitation of certain stretch and bend vibrations. This behaviour resembled closely that found in HF and permitted the assignment of the structure to vibrational Feshbach resonances. An attempt to associate the structures observed in CS_2 with vibrational thresholds is represented by the grids and bars indicating selected vibrational levels of neutral CS_2 in figure 2. The grids coincide with the observed structures in some cases but not in others. The spacings of the observed structures are reminiscent of the bending and symmetrical stretch vibrational frequencies of neutral CS_2, but an entirely satisfactory assignment of the structures to vibrational thresholds does not appear possible. (The only exception is the assignment of three minima in the total cross section to thresholds for the excitation of the fundamental vibrations of CS_2 made by Jones *et al* (2002).)

An alternative approach would be to attempt to assign the peaks in the spectra to progressions of quasistationary vibrational states of CS_2^- with origins below zero. A spacing of about 38 meV is frequently found in the spectra of figure 2 and could correspond to a bending frequency of the anion (ν_2 of neutral CS_2 is 49 meV). Many peaks could be assigned to progressions in this frequency. For example, the peaks in the elastic cross section could be assigned to a progression with a spacing of about 40 meV and origin around -20 meV. This could be the origin of either the $^2B_2$ branch of the valence, or of a diffuse state of CS_2^-. A satisfactory empirical assignment of the observed peaks to progressions of bending and stretch vibrations of a valence state of CS_2^- does not appear possible, however. Part of the problem is that the vibrational frequencies of CS_2^- are low, the density of the possible overtone and combination vibrations high, and many alternative assignments are possible; none of which is entirely convincing. A further complication is the expected spin–orbit splitting of CS_2^-. The (010) cross section has three doublets of peaks separated by about 14 meV, an energy which could correspond to the spin–orbit splitting. A conclusive assignment is not possible, however, because this splitting does not appear consistently in all the spectra and could also be of vibrational origin. The conclusion is thus that the situation in CS_2 is more complex than in CO_2. The observed structures cannot be satisfactorily and uniquely explained by a single diffuse state of CS_2^- whose potential surface mimics that of the neutral CS_2 at low energies as was the case in CO_2, and a detailed empirical assignment to vibrational levels of a valence state of CS_2^- also fails.

Rosmus and Hochlaf (2002) calculated the vibrational states of CS_2^- at a very high degree of sophistication, including both the $^2A_1$ and $^2B_2$ states, anharmonicities, Renner–Teller effect and spin–orbit splitting. Their method has proven highly successful in the interpretation of the vibrational structure of CS_2^+ in very high resolution photoelectron spectra (Liu *et al* 2001).

In the case of CS_2^- the calculation yielded a very complex structure of often irregular, highly mixed, densely spaced levels. Their calculation ignores the fact that the present vibrational levels are resonances coupled to continuum, but this neglect is not dramatic because the narrow width of the observed structures indicates that the coupling is not very strong. Comparison of their calculation with the present spectra was hampered by several problems and did, unfortunately, not lead to a useful assignment. The problems were as follows.

- The energies of the origins of the $^2A_1$ and $^2B_2$ states (i.e. the adiabatic and the vertical electron affinities) are not known precisely enough.
- The structures observed in the present spectra are a substantial amount of energy (about 1 eV for the $^2A_1$ state) above the origins of the electronic states. The density of the calculated vibrational levels is already very high here, with average spacing less than the resolution of the present experiment.
- The present experiment lacks the very restrictive, clearly defined selection rules which facilitated the assignment of the photoelectron spectrum.

The calculation is very useful despite the failure of a detailed assignment. It shows that the vibrational structure of the valence states of CS_2^- is expected to be very complex and in part irregular, and that the present failure to assign the observed structures to simple progressions is compatible with their results for the $^2A_1$ and $^2B_2$ states.

Experimental information on the vibrations of CS_2^- is provided by the infrared absorption measurements of matrix trapped CS_2^- by Zhu and Andrews (2000), who obtained a frequency of 144 meV. This is substantially lower than 190 meV, the ν_3 antisymmetrical stretch frequency of neutral CS_2. The bending and symmetrical stretch vibrations appear to be more active in the present experiment than the antisymmetrical stretch, however, and no direct correlation of the two experiments is possible.

3.3. Overtone and combination vibrations

Figure 3 shows cross sections for the excitation of various overtone and combination vibrations. The density of vibrational states at these energies is already quite high and the cross sections are less precise than those for the fundamental vibrations because of band overlap. In addition, the experiment cannot resolve the $(02^00)(\Sigma)$ and $(02^20)(\Delta)$, and the $(03^10)(\Pi)$ and $(03^30)(\Phi)$ vibrational states and the data given is the sum of the cross sections. The cross sections have the same pronounced structure as those for the fundamental vibrations, but the structure does not become deeper as was the case in CO_2. As already mentioned in connection with the energy-loss spectra, the cross sections do not drop with increasing final vibrational quantum as fast as was the case in the threshold region of CO_2.

3.4. Superelastic scattering

Figure 4 shows three superelastic cross sections. These cross sections do not provide fundamentally new scientific information because they are related to the corresponding inelastic cross sections by the detailed balance principle. They represent a useful test of the consistency of the experiment, however. Figure 5 compares the cross section measured on the $(100) \rightarrow (000)$ superelastic peak with that derived from the experimental $(000) \rightarrow (100)$ cross section using the detailed balance relation. The two sets of data agree well for energies larger than about 160 meV, but the actually measured cross section becomes increasingly smaller at lower energies. It is important to realize that the incident electron energy is 82 meV at the threshold of the inelastic measurement, whereas it is zero at the threshold of the superelastic

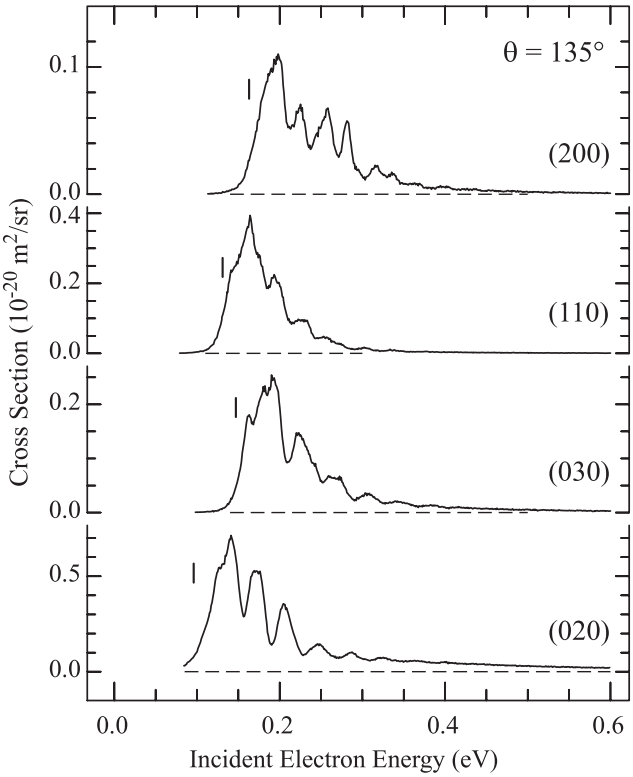

Figure 3. Differential cross sections for overtone and combination vibrations.

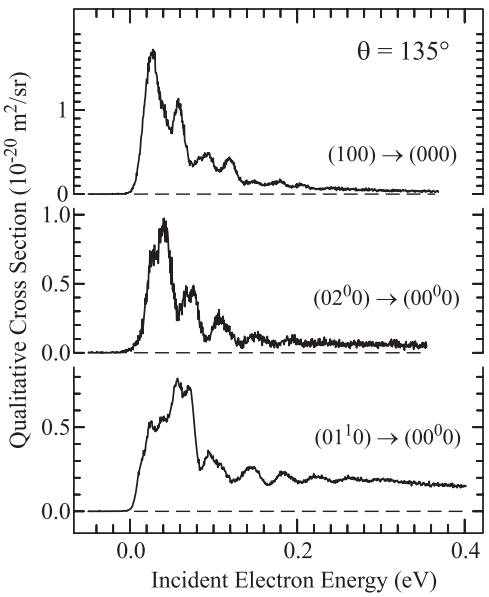

Figure 4. Superelastic cross sections from thermally excited vibrational states. The magnitudes are only qualitative below about 0.2 eV—see text.

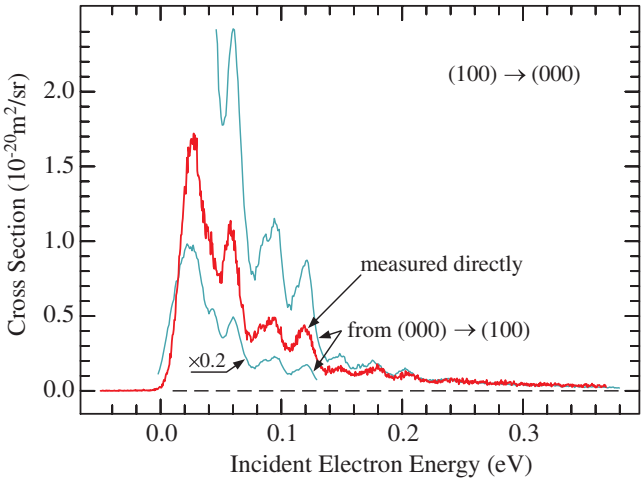

Figure 5. The superelastic (100) → (000) cross section calculated from the experimental (000) → (100) inelastic cross section using the detailed balance relationship and measured directly.

measurement. The superelastic measurement is thus harder to perform since it requires lower incident energies. The discrepancy between the two data sets is presumably due to the fact that the incident electron beam becomes increasingly diffuse at energies below about 200 meV, reducing the signal. The present correction scheme for the instrumental response function does not account for this effect. The superelastic cross sections may provide means of improving the method of response function correction at very low energies in the future, however. The shape of the structures is identical in the elastic and inelastic data, confirming the reliability of the experiment in this respect.

Application of the detailed balance principle to the (000) → (020) transition is complicated by the fact that the two final states $(02^00)(\Sigma)$ and $(02^20)(\Delta)$ overlap and the repartition of the two cross sections to the observed signal is not known *a priori*. Reasonable agreement between the directly measured superelastic transition and that derived via the detailed balance relation (figure 6) is obtained only when the population of the thermally excited (020) state is calculated under the assumption that this state is not degenerate, that is, that it is only the not degenerate (02^00) state which contributes. This is an experimental indication that $\Sigma \rightleftharpoons \Sigma$ transitions dominate over $\Sigma \rightleftharpoons \Delta$ transitions.

4. Cross sections at higher energies

Figure 7 shows the cross sections from the near-threshold region till 12 eV on a log–log scale. The present values of the cross sections agree quite well with those of Sohn *et al* (1987) at energies above 1 eV, but are somewhat larger below 1 eV. A number of resonances can be discerned. They are most pronounced in the (100) cross section, where bands appear at 3.65, 7.8 and 9.6 eV. All three values correspond to peaks of S^- production in the dissociative electron attachment spectrum (Ziesel *et al* 1975, Dressler *et al* 1987, Krishnakumar and Nagesha 1992). They have been assigned to core-excited resonances (Dressler *et al* 1987, Pogulay *et al* 1994). Broad bands further appear at 2, 5, 7 and 10 eV in the (001) cross section, and at 4.5 and 10 eV in the (010) cross section. There has been discussion whether there is a resonance around 2 eV (Szmytkowski 1987). There is no evidence for such a resonance in the present elastic cross section, but a weak broad band peaking around 2 eV appears in the (001) cross section.

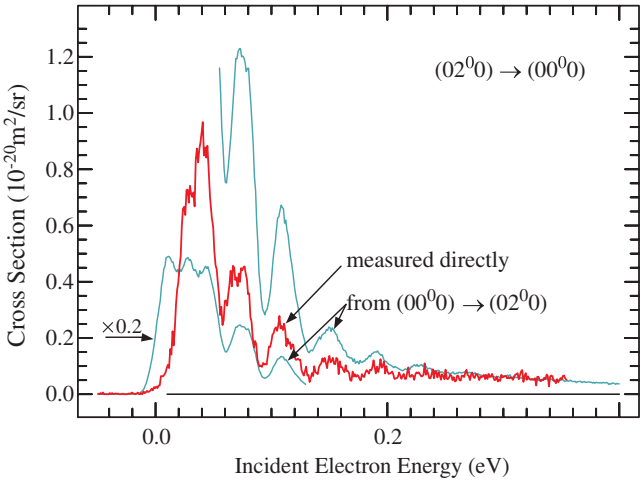

Figure 6. The superelastic (02^{0}0) → (000) cross section calculated from the experimental (000) → (02^{0}0) inelastic cross section using the detailed balance relationship and measured directly.

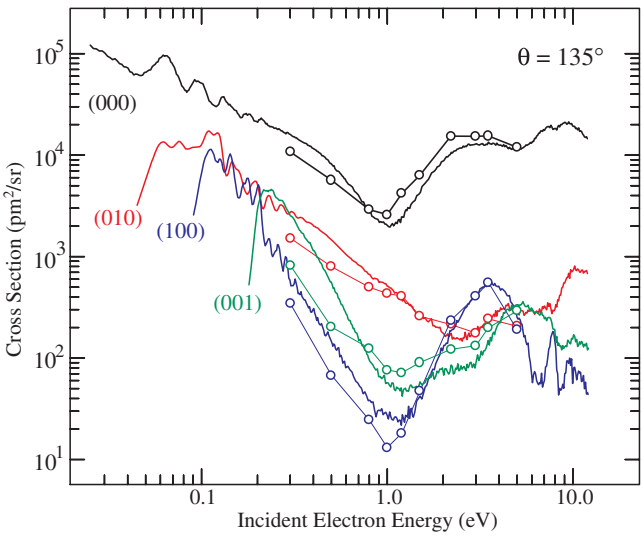

Figure 7. The differential cross sections shown over a larger range of electron energies on a log–log scale. Curves show the present data, circles connected by straight lines the cross sections of Sohn *et al* (1987), interpolated between 130° and 138°. Topmost curve and circles show the elastic cross section, the lower three curves show the cross sections for the excitation of the fundamental vibrations as indicated.

5. Discussion

Near threshold structures in hydrogen halides and CO_2 are caused by vibrational Feshbach resonances supported by anionic states with spatially diffuse wavefunctions, where an electron is weakly bound by a combination of dipole, quadrupole and polarization forces at distorted (stretched and bent) molecular geometries, and becomes unbound in the vicinity of the neutral equilibrium geometry (Allan *et al* 2000, Čížek *et al* 2001, 2003, Knoth *et al* 1989, Allan 2002).

The structures in the CS_2 cross sections are undoubtedly also caused by vibrational activity, that is, correspond to quasistationary vibrational levels of the negative ion. It is much harder, however, to assign the electronic state of the anion on which this vibrational activity takes place because the $^2\Pi_u$ valence state, which is a shape resonance at 3.6 eV in CO_2, lies lower in CS_2 and is likely to strongly influence scattering in the near-threshold region. The vertical electron affinity corresponding to the $^2\Pi_u$ state in the linear geometry is around 0 eV (Oakes and Ellison 1986, Gutsev *et al* 1998, Bettega 2000). This state splits into $^2A_1$ and $^2B_2$ branches upon bending. The minimum of the $^2A_1$ branch corresponds to the adiabatic electron affinity, the experimental and theoretical results for which range between about +0.3 and +0.9 eV (Dispert and Lacmann 1975, Gutsev *et al* 1998 and references therein). The $^2A_1$ and $^2B_2$ states of CS_2^- are bound states at low energies and become shape resonances at energies accessible in a scattering experiment. High vibrational levels on both branches of the $^2\Pi_u$ state of CS_2^- lie in the same energy range as the structures in the cross sections and could be responsible for them, apart from a 'diffuse' state which has been invoked to explain the structures in CO_2.

The existence of a diffuse state in CS_2^- is uncertain. It has been postulated by Kalamarides *et al* (1988) on experimental grounds—the observation of field-induced detachment from CS_2^- formed in Rydberg atom collisions with CS_2. Two field autodetaching states have been observed to result from Rydberg electron transfer by Suess *et al* (2003). The theoretical work of Compton *et al* (1996) invoked quadrupole binding to explain the observations. On the other hand Gutsev *et al* (1998) calculated the dipole moment of bent CS_2 to be rather small (0.46 D at the CS_2^- equilibrium geometry, compared to -0.9 D for CO_2) and did not find any diffuse dipole or quadrupole bound states in their calculations. They propose that the field-detachment results can be explained by the nearly linear configuration of CS_2^-. In favour of the existence of a diffuse state there is the fact that structures due to a diffuse state were recently observed in even CO_2, which is substantially less polarizable. If it does exist, however, then the situation is much more complex than in CO_2 because it would mix with the $^2A_1$ valence state present in CS_2^- at low energies, giving rise to avoided crossings and conical intersections, and consequently to very complicated adiabatic surfaces and strong nonadiabatic effects in nuclear motion.

Barsotti *et al* (2002) measured electron attachment to CS_2 clusters under very high resolution and found no sharp structures due to vibrational Feshbach resonances. This observation is intriguing in view of the fact that many sharp structures were found for isolated CS_2 molecules in this work and the fact that in the case of CO_2 and N_2O vibrational Feshbach resonances were found both in clusters (Barsotti *et al* 2002, Leber *et al* 2000) and in isolated molecules (Allan 2002, 2003).

6. Conclusions

A wealth of sharp structures was observed in the elastic and the vibrationally inelastic cross sections in CS_2. The narrow width indicates that the associated decays are relatively slow. The structures could not be uniquely assigned to vibrational Feshbach resonances lying just below vibrational thresholds and supported by a diffuse dipole and polarization force bound state of CS_2^-. They are more consistent with the explanation of quasistationary vibrational levels of the $^2\Pi_u$ valence state with its $^2A_1$ and $^2B_2$ branches. This state has a calculated vertical electron affinity of about zero, that means that the lower part of its Franck–Condon envelope is a bound state, but the upper part is a shape resonance analogous to the 3.6 eV shape resonance of CO_2. The autodetachment lifetime of shape resonances is generally longer when they lie at lower energies, explaining why the present structures are narrower than the boomerang structures around 3.6 eV in CO_2. Substantial excitation of vibrational overtones,

a frequent characteristics of a low-lying π^* shape resonances, is observed even very close to the threshold, and represents an additional indication of the dominant role of the valence state of CS_2^-. The $^2\Pi_u$ state is also likely to be responsible for the very high threshold peaks. A contribution of a diffuse dipole and polarization force bound state of CS_2^- cannot be excluded, however, and appears plausible in view of the results in the less polarizable molecule CO_2. Substantial vibronic mixing of the valence and the diffuse state could then ensue, leading to complicated adiabatic potential surfaces.

The present spectra also illustrate the capacity of the cross beam technique to measure cross sections over wide energy ranges. Together with the 'magnetic angle changer' technique of Read and co-workers (Zubek *et al* 1996) such spectra could be measured at a number of scattering angles and integrated to yield (nearly) assumption-free integral and momentum-transfer cross sections.

Acknowledgments

The author is grateful to P Rosmus and M Hochlaf for communicating the unpublished results of their CS_2^- vibration calculation. This research is part of project no 2000-067877.02 of the Swiss National Science Foundation.

References

Allan M 1992 *J. Phys. B: At. Mol. Opt. Phys.* **25** 1559
Allan M 1995 *J. Phys. B: At. Mol. Opt. Phys.* **28** 5163
Allan M, Čížek M, Horáček J and Domcke W 2000 *J. Phys. B: At. Mol. Opt. Phys.* **33** L209
Allan M 2001a *Phys. Rev. Lett.* **87** 033201
Allan M 2001b *Int. Symp. on Electron–Molecule Scattering and Swarms (EMS01) (Lincoln, USA)* p 147 (Abstracts)
Allan M 2001c *ICPEAC: Proc. 22nd Int. Conf. on the Photonic Electronic and Atomic Collisions (Santa Fe, USA, 2001)* p 275 (Abstracts of contributed papers)
Allan M 2002 *J. Phys. B: At. Mol. Opt. Phys.* **35** L387–95
Allan M 2003 *J. Phys. B: At. Mol. Opt. Phys.* submitted
Barsotti S, Leber E, Ruf M-W and Hotop H 2002 *Int. J. Mass Spectrom.* **220** 313
Bettega M H F 2000 *Aust. J. Phys.* **53** 785
Čížek M, Horáček J, Allan M, Sergenton A-C, Popović D B, Domcke W, Leininger T and Gadea F X 2001 *Phys. Rev.* A **63** 062710
Čížek M, Horáček J, Allan M and Fabrikant I I 2003 *J. Phys. B: At. Mol. Opt. Phys.* at press
Compton R N, Dunning F B and Nordlander P 1996 *Chem. Phys. Lett.* **253** 8
Dispert H and Lacmann K 1975 *Ber. Hahn-Meitner-Inst. Kernforsch. Berlin* **198** 34
Dressler R A, Allan M and Tronc M 1987 *J. Phys. B: At. Mol. Phys.* **20** 393
Estrada H and Domcke W 1985 *J. Phys. B: At. Mol. Phys.* **18** 4469
Field D, Lunt S L, Mrotzek G, Randell J and Ziesel J P 1991 *J. Phys. B: At. Mol. Opt. Phys.* **24** 3497
Gutsev G L, Bartlett R J and Compton R J 1998 *J. Chem. Phys.* **108** 6756
Gopalan A, Bömmels J, Götte S, Landwehr A, Franz K, Ruf M-W, Hotop H and Bartschat K 2003 *Eur. Phys. J.* D **22** 17
Hotop H, Ruf M-W, Allan M and Fabrikant I I 2003 *Adv. At. Mol. Opt. Phys.* at press
Johnstone W M, Mason N J and Newell W R 1993 *J. Phys. B: At. Mol. Opt. Phys.* **26** L147
Johnstone W M, Brunger M J and Newell W R 1999 *J. Phys. B: At. Mol. Opt. Phys.* **32** 5779
Jones N C, Field D, Ziesel J-P and Field T A 2002 *Phys. Rev. Lett.* **89** 093201
Kalamarides A, Walter C W, Smith K A and Dunning F B 1988 *J. Chem. Phys.* **89** 7226
Knoth G, Gote M, Rädle M, Jung K and Ehrhardt H 1989 *Phys. Rev. Lett.* **62** 1735
Kochem K H, Sohn W, Nebel N, Jung K and Ehrhardt H 1985 *J. Phys. B: At. Mol. Phys.* **18** 4455
Krishnakumar E and Nagesha K 1992 *J. Phys. B: At. Mol. Opt. Phys.* **25** 1645
Leber E, Barsotti S, Bömmels J, Weber J M, Fabrikant I I, Ruf M-W and Hotop H 2000 *Chem. Phys. Lett.* **325** 345
Lide D R (ed) 1995 *CRC Handbook of Chemistry and Physics* 76th edn (Boca Raton, FL: Chemical Rubber Company Press)

Liu J, Hochlaf M, Chambaud G, Rosmus P and Ng C Y 2001 *J. Phys. Chem.* A **105** 2183
Morgan L A 1998 *Phys. Rev. Lett.* **80** 1873
Nesbet R K 1979 *Phys. Rev.* A **20** 58
Oakes J M and Ellison G B 1986 *Tetrahedron* **42** 6263
Pogulay A V, Muftakhov M V and Khvostenko V I 1994 *J. Electron. Spectrosc. Relat. Phenom.* **70** 95
Rohr K and Linder F 1976 *J. Phys. B: At. Mol. Phys.* **9** 2521
Rosmus P and Hochlaf M 2002 private communication
Sohn W, Kochem K-H, Scheuerlein K M, Jung K and Ehrhardt H 1987 *J. Phys. B: At. Mol. Phys.* **20** 3217
Sommerfeld T 2003 *J. Phys. B: At. Mol. Opt. Phys.* **36** L127
Suess L, Parthasarathy R and Dunning F B 2003 *Chem. Phys. Lett.* **372** 692
Szmytkowski C Z 1987 *J. Phys. B: At. Mol. Phys.* **20** 6613
Tennysson J and Morgan L 1999 *Phil. Trans. R. Soc.* A **357** 1161
Zhu M and Andrews L 2000 *J. Chem. Phys.* **112** 6576
Ziesel J P, Schulz G J and Milhaud J 1975 *J. Chem. Phys.* **62** 1936
Zubek M, Gulley N, King G C and Read F H 1996 *J. Phys. B: At. Mol. Opt. Phys.* **29** L239